Research
Diversified Food Supply System—Article

Plant Factory Speed Breeding Significantly Shortens Rice Generation Time and Enhances Metabolic Diversity

Yi Liu [a,b,#], Zong-Geng Li [a,#], Hao Cheng [a], Xiao Yang [a], Ming-Yue Li [a,c], Hong-Yan Liu [a,*], Ren-You Gan [d,*], Qi-Chang Yang [a,*]

[a] Institute of Urban Agriculture, Chinese Academy of Agricultural Sciences, National Agricultural Science & Technology Center, Chengdu 610213, China
[b] Nutrition and Bromatology Group, Department of Analytical and Food Chemistry, Faculty of Science, Universidade de Vigo, Ourense 32004, Spain
[c] Key Laboratory of Coarse Cereal Processing (Ministry of Agriculture and Rural Affairs), Sichuan Engineering & Technology Research Center of Coarse Cereal Industrialization, School of Food and Biological Engineering, Chengdu University, Chengdu 610106, China
[d] Department of Food Science and Nutrition, Faculty of Science, The Hong Kong Polytechnic University, Hong Kong 999077, China

ARTICLE INFO

ABSTRACT

Rice (*Oryza sativa* L.) plays a pivotal role in global food security, yet its breeding is constrained by its long generation time and seasonality. To enhance rice breeding efficiency and meet future food demands, we have developed a vertical hydroponic breeding system integrated with light-emitting diodes (LEDs) lighting in a closed plant factory (PF), which significantly accelerates rice growth and generation advancement. The results show that indica rice can be harvested as early as after 63 days of cultivation, a 50% reduction compared with field cultivation, enabling the annual harvesting of 5–6 generations within the PF. A hyperspectral imaging (HSI) system and attenuated total reflectance infrared (ATR-IR) spectroscopy were further employed to characterize the chemical composition of the PF- and field-cultivated rice. Metabolomics analysis with ultra-performance liquid chromatography-tandem mass spectrometry (UPLC-MS/MS) and gas chromatography-mass spectrometry (GC-MS) revealed that, compared with the field-cultivated rice, the PF-cultivated rice exhibited an up-regulation of total phenolic acids along with 68 non-volatile and 19 volatile metabolites, such as isovitexin, succinic acid, and methylillicinone F. Overall, this study reveals the unique metabolic profile of PF-cultivated rice and highlights the potential of PFs to accelerate the breeding of crops such as rice, offering an innovative agricultural strategy to support food security in the face of global population growth and climate change.

1. Introduction

Rice (*Oryza sativa* L.) is a staple food for more than 60% of the world's population, playing a pivotal role in global food security, nutrition, and economics [1–5]. By 2050, the global population may reach ten billion [6], leading to a huge requirement for rice to support the increased population [7,8]. However, conventional rice breeding is time-consuming and inefficient, and thus cannot meet the demands of the huge global population in the future [9]. Moreover, it remains a challenge to quickly develop new varieties of rice with high yield and high quality to keep up with the pace of future demand. Therefore, the research and development of "speed-breeding" technologies can be important for enhancing the breeding efficiency of crops—especially rice—in order to guarantee future global food security.

Fully environment-controlled facilities, such as growth chambers, have been applied to accelerate crop breeding through environmental control [10,11]. A plant factory (PF) is an indoor, advanced, and intensive form of hydroponic production system, in which the growing environment, including the rhizosphere, is optimally controlled to accelerate the development rate of plants and increase the harvest frequency per year in comparison with traditional field cultivation [12]. Speed breeding has been successfully used to enhance the generation advancement of certain long-day crops, such as spring wheat (*Triticum aestivum*), durum wheat (*T. durum*), barley (*Hordeum vulgare*), chickpea (*Cicer arietinum*), and pea (*Pisum sativum*) [13,14], but it has not been successfully applied to short-day crops such as rice, due to the challenge of flowering inhibition caused by the prolonged photoperiod. To sig-

* Corresponding authors.
E-mail addresses: liuhongyan01@caas.cn (H.-Y. Liu), renyou.gan@polyu.edu.hk (R.-Y. Gan), yangqichang@caas.cn (Q.-C. Yang).
# These authors contributed equally to this work.

nificantly shorten the long process of developing suitable varieties, speed breeding protocols based on light-emitting diodes (LEDs) have been introduced for short-day crops [15,16]. A speed-breeding protocol named SpeedFlower was reported to induce speed flowering of rice mainly through control of the light spectrum, light intensity, and photoperiod in a fully controlled facility; combined with premature seed harvesting and gibberellin A3 (GA3) treatment, the protocol achieved 4–5 generations of rice within a year [16]. However, that protocol did not consider the impact of the rhizosphere on rice speed breeding.

Speed breeding can not only significantly shorten the growth period of rice but also affect its metabolic profiles. Nevertheless, the specific metabolic changes in PF-cultivated rice with a shortened growth period remain unclear. Recently, both a hyperspectral imaging (HSI) system and attenuated total reflectance (ATR) infra-red (IR) spectroscopy have been demonstrated to have potential applications in obtaining the spectral information of seeds in order to analyze their internal chemical components, such as protein and starch [3,17]. In addition, metabolomics analysis using ultra-performance liquid chromatography-tandem mass spectrometry (UPLC-MS/MS) and gas chromatography-mass spectrometry (GC-MS) is a reliable method to evaluate food quality by identifying distinct metabolites [18,19]. Therefore, obtaining key spectral and metabolomic information of rice can be valuable for its quality evaluation.

In this study, we established a vertical multilayer hydroponic breeding system in a closed PF to accelerate rice breeding through manipulation of the growing environment, especially LED lighting. To clarify the impact of PF cultivation on rice quality, we employed ATR-IR and an HSI system, as well as metabolomic analyses using UPLC-MS/MS and GC-MS, to systematically investigate the quality of PF-cultivated rice in comparison with field-cultivated rice. We expect this study will provide an innovative strategy to advance breeding technologies by enhancing breeding efficiency, while supporting the fast production of a crop to guarantee global food security.

2. Materials and methods

2.1. Rice materials and chemicals

An indica rice variety (ZF802M) with a wide planting area in South China was selected for PF cultivation in this study. Sodium chloride (NaCl) was purchased from Sinopharm Chemical Reagent Co., Ltd. (China). Potassium bromide (KBr) and *n*-hexane were purchased from Jinpan Biotechnology Co., Ltd. (China). Methanol, ace-tonitrile, ammonium acetate, and formic acid (high performance liquid chromatography (HPLC) grade) were bought from Kelong Chemical Reagent Factory (China). All other reagents were of analytical grade.

2.2. Speed breeding of rice

First, the seeds were soaked in the water at 28 °C for 24 h; then, they were transferred into a nursery tray. After seedlings emerged, the tray was placed under LED light (TYF Co., Ltd., China) with a white–red–blue chip ratio of 1:1:1 for 7 d. The spectrum of the white LED light consisted of blue light (28%), green light (42%), red light (28%), and far red and ultraviolet (UV) light (2%) (Fig. 1(a)). The photon flux density (PFD) was set at 100 $\mu mol \cdot m^{-2} \cdot s^{-1}$ (10 cm above the tray) for 13 h (7:00–20:00) a day, and the proportions of red, blue, green, and far-red and UV light were 35%, 47%, 16.5%, and 1.5%, respectively (Fig. 1(b)). Next, the rice seedlings were transported to a double-layer hydroponic cultivation system with a panel of LED lights. The cultivation board was 120 cm long and 60 cm wide, with 18 holes on each board, and three rice seedlings were cultivated in each hole. The distance from the LED light to the cultivation board was 60 cm, and the PFD was 350 $\mu mol \cdot m^{-2} \cdot s^{-1}$ (10 cm above the cultivation board). The spectral composition of the LED light is shown in Fig. 1(b); the photoperiod (Table S1 in Appendix A) was dynamically regulated to accelerate the growth of rice. Hoagland's solution (pH (6.3 ± 0.1); electrical conductivity (1.6 ± 0.1) $mS \cdot cm^{-1}$) was used for rice cultivation, and the nutrient solution was recirculated all day by means of a 60-W pump to improve the concentration of dissolved oxygen (DO). During the whole cultivation period, the indoor day/night air temperature was set to (28/21 ± 2) °C, and the relative air humidity was adjusted to (65% ± 5%) for the entire day. The carbon dioxide concentration was set to (400 ± 10) $\mu mol \cdot mol^{-1}$ in the daytime. The harvested rice was dried under sunlight and stored in a refrigerator at 4 °C.

2.3. Hyperspectral image acquisition

Hyperspectral technology was applied to differentiate the PF- and field-cultivated rice seeds according to previous studies, with some modifications [20,21]. Before image acquisition, 30 randomly selected rice seeds of each sample were placed on a blackboard (Fig. 2(a)). An HSI system with wavenumbers between 400 and 1000 cm^{-1} was utilized to acquire full continuous spectral images of rice seed samples in the reflectance mode. The parameters for image acquisition are shown in Table S2 in Appendix A. Images
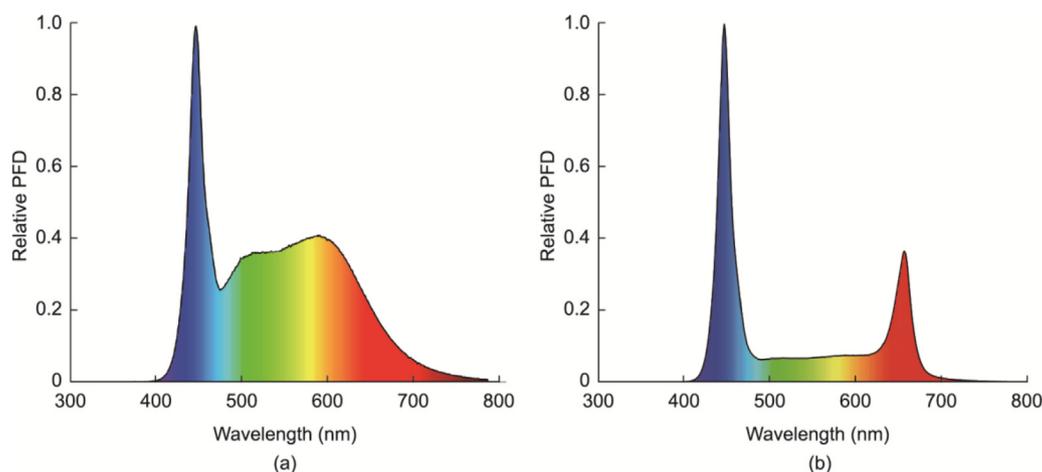

Fig. 1. Spectral composition of the LED light. (a) Spectral composition of white LED light; (b) spectral composition of white + blue + red LED light.

and hyperspectral reflectance data of the PF- and field-cultivated rice seeds were then acquired. To improve the comparability and robustness of the image acquisition, two extra images—a dark-current image (R_D) and a white reference image (R_W)—were used to adjust the original images (R_0) acquired of the rice seed samples. The R_D, with about 0 diffuse reflectance, was obtained by covering the camera lens with an opaque lid, while the R_W, with about 99.9% diffuse reflectance, was acquired from a white board. Adjustment of all images was performed using SpectrononPro 3.0.3 software (Resonon Inc., USA). The adjusted images (R) of the rice seed samples were calculated using the following equation:

$$R = \frac{(R_0 - R_D)}{(R_W - R_D)}$$

Finally, a combination of principal component analysis (PCA) and orthogonal partial least-squares discriminant analysis (OPLS-DA) was used to analyze the spectral information of the rice seeds.

2.4. ATR-IR spectra acquisition

Rice seed samples (with hulls) were dried in an oven at 38 °C until free of moisture and then milled into fine powder for the acquisition of ATR-IR spectra. In brief, 1.5 mg of the rice powder sample was thoroughly mixed with 150 mg of KBr, and the mixture was then pressed into sheets. KBr (150 mg) without rice powder was also pressed into a sheet as a blank control. The sheet samples were then fixed on the ATR germanium crystal for spectrum acquisition with single reflection at an angle of 45°. The blank sheet was used to acquire a reference background spectrum. The ATR-IR was set at a spectrum wavenumber range between 400 and 4000 cm^{-1}, resolution of 4 cm^{-1}, scanner frequency of 7.5 kHz, and scan number of 32 times at 25 °C. OMNIC 8.0 software (Thermo Fisher Scientific Inc., USA) was used for spectral acquisition. Spectrum analysis was conducted in triplicate for each sample. To compare the spectral differences of PF- and field-cultivated rice seeds, PCA and OPLS-DA were conducted on the ATR-IR spectra data of each sample.
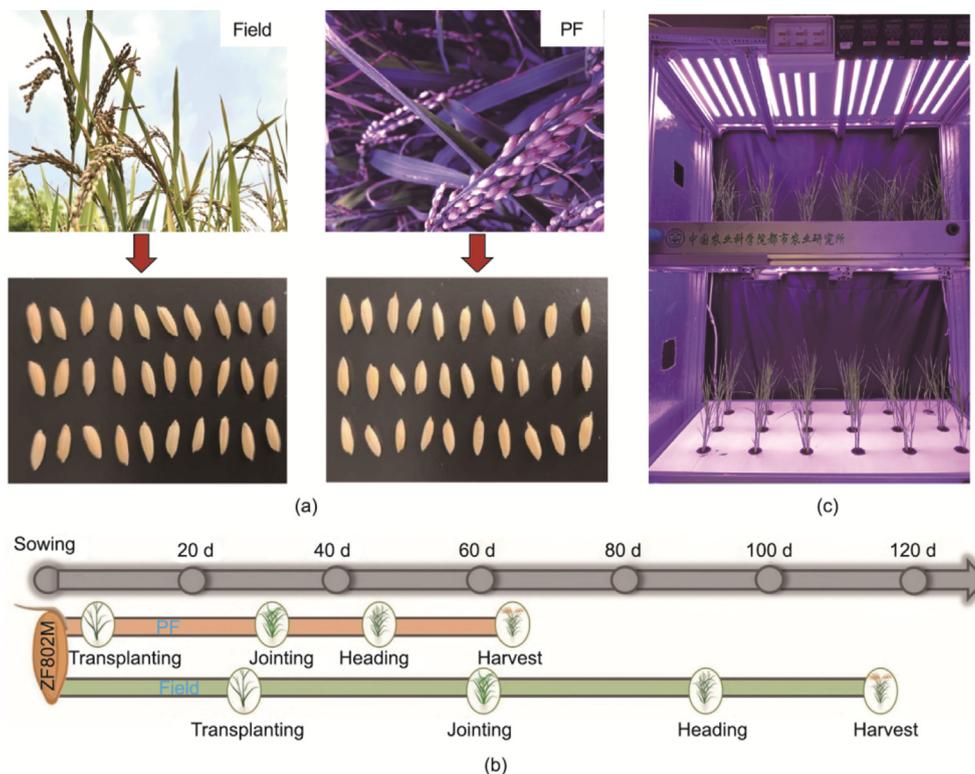
2.5. Widely targeted metabolomics analysis of non-volatiles by UPLC-MS/MS

2.5.1. Sample preparation

Rice seeds were dried through lyophilization, milled into fine powder, and then extracted, according to the method reported in a previous study [22]. In brief, the rice seed powder (50 mg) was mixed with 1.2 mL of 70% methanol aqueous solution at room temperature, which was then vortexed six times, with each time being for 30 s per 30 min. After centrifugation (12 000g, 3 min), the supernatant was collected, filtered (0.22-μm pore size), and subjected to UPLC-MS/MS analysis.

2.5.2. UPLC-MS/MS conditions

UPLC-MS/MS analysis was performed based on the method reported in a previous study [23]. Sample separation was carried out using a SHIMADZU Nexera X2 UPLC system (Shimazu, Japan) equipped with an Agilent SB-C18 column (1.8 μm, 2.1 mm × 100 mm). The mobile phase consisted of solvent A (0.1% formic acid aquatic solution) and solvent B (0.1% formic acid in acetonitrile). The mobile phase gradient program was set as follows: 0 min, 5% solvent B; 0–9 min, 5% to 95% solvent B, 9–10 min, 95% solvent B; 10–11.10 min, 95% to 5% solvent B; 11.10–14 min, 5% solvent B. The column temperature was set at 40 °C, and the injection volume was 4 μL under a flow rate of 4.0 mL·min^{-1}. Furthermore, the tandem quadrupole (QQQ) and linearion trap (LIT) modes were acquired with an Applied Biosystems 4500 triple QTRAP System (Thermelfeld, USA) equipped with an electrospray ionization (ESI) Turbo Ion-Spray interface. The ESI parameters were set as follows: source temperature, 550 °C; ion spray voltage, 5500 V (positive)/–4500 V (negative); ion source gas I, 50 psi and gas II, 60 psi; and curtain gas, 25 psi. A quality control (QC) sample was used by

Fig. 2. The PF speed-breeding system for rice seeds. (a) Pictures of PF- and field-cultivated rice seeds; (b) growth cycle of PF- and field-cultivated rice seeds; (c) picture of rice speed breeding.

mixing an equal amount of each single sample to analyze the repeatability of samples under the same treatment method.

2.6. GC-MS analysis of volatile metabolites

2.6.1. Sample preparation

Frozen rice seeds (stored at −80 °C) were ground with liquid nitrogen and mixed evenly by vortex. A sample of about 500 mg in 1 mL of liquid nitrogen was placed into the headspace bottle, followed by the addition of saturated NaCl solution (10 μL, 50 μg·mL^{-1}); the mixture was extracted by means of fully automated headspace solid-phase micro-extraction (HS-SPME). In brief, the mixture was incubated at 60 °C for 5 min, extracted using a 120-μm SPME fiber assembly of divinylbenzene/carboxen/polydi methylsiloxane (DVB/CAR/PDMS) for 15 min, kept at 250 °C for 5 min, and then subjected to GC-MS analysis. Before sampling, the extraction head was aged for 5 min at 25 °C in the fiber conditioning station.

2.6.2. GC-MS conditions

An Agilent 8890/7000D GC-MS was used to analyze volatile metabolites. A sample extracted by means of HS-SPME was separated using a DB-5ms capillary column (30 m × 0.25 mm × 0.25 μm) (Agilent J&W Scientific, USA). The temperature program was set at 40 °C from 0–3.5 min, increased to 100 °C at 10 °C ·min^{-1}, increased to 180 °C at 7 °C ·min^{-1}, then increased to 280 °C at 25 °C ·min^{-1}, and finally maintained at 280 °C for 5 min. The nitrogen was set at a flow rate of 1.2 mL·min^{-1}, and the solvent was delayed for 3.5 min. The mass spectrometry (MS) analysis was performed in single ion monitoring (SIM) mode and qualitative and quantitative ion accurate scanning mode, and the MS electron energy was 70 eV. The quadrupole temperature, mass spectrum interface temperature, and ion source temperature were set at 150, 280, and 230 °C, respectively. Compounds were tentatively identified by comparing the similarity of their fragmentation with those in the National Institute of Standards and Technology (NIST) library. A mixture of 1 μL of *n*-alkane (C7–C25) was run under the same capillary column and GC-MS conditions to obtain the Kovats' retention indices (RIs).

2.7. Statistical analysis

The spectral data and bar charts were created using Origin 2022 (OriginLab, USA). Hierarchical cluster analysis (HCA), PCA, and OPLS-DA of the primary and secondary metabolites of the rice seeds were conducted using Cloud platform tools from a web-based platform. Variable importance in projection (VIP) ≥ 1 combined with a fold change (FC) ≥ 2 and FC ≤ 0.5, based on the OPLS-DA model, was used for filtering the differential metabolites between samples. A visualized metabolic map of the main metabolites and related metabolic pathways was presented in Section 3.4.2 based on the Kyoto Encyclopedia of Genes and Genomes (KEGG).

3. Results and discussion
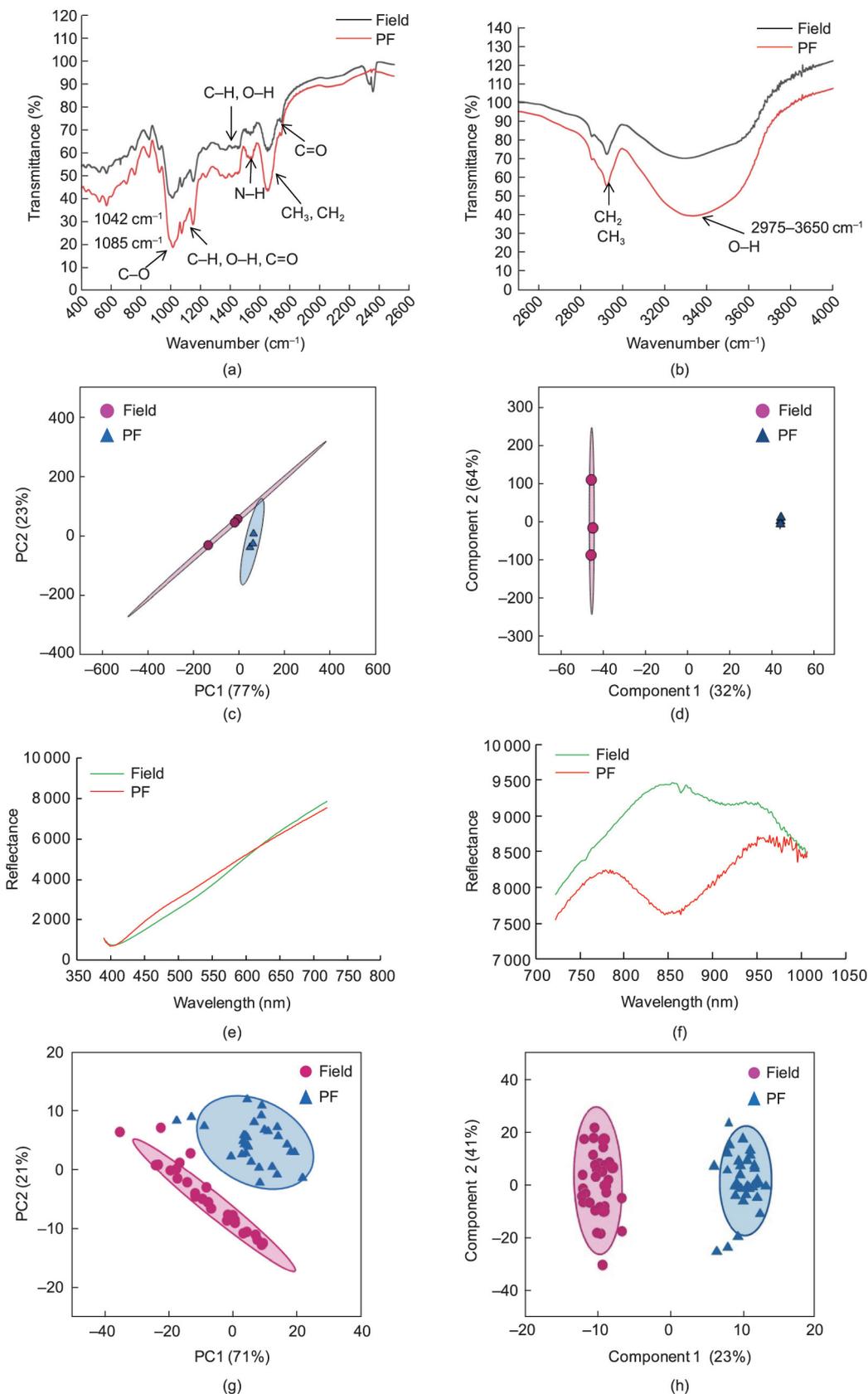
3.1. PF-accelerated rice breeding

As shown in Fig. 2(b), the Indica variety (ZF802M) of rice started heading on the 45th day and was harvested on the 63rd day after transplantation. Compared with the field cultivation, the growth period of ZF802M in the PF was generally shortened by half, such that 5–6 generations of rice could be achieved in one year. The seed-setting rate and grain-straw ratio of rice in the PF were 87.8% and 0.60, respectively. Moreover, the seeds were highly vigorous after being harvested from the PF, with a germination rate higher than 96% and a 1000-grain weight of (25.0 ± 0.2) g.

Compared with previous studies on speed breeding [15,16,24–26], we propose a vertical multilayer hydroponic breeding system in a PF for the first time (Fig. 2(c)). The hydroponic system can ensure adequate nutrient supply, improve fertilizer utilization efficiency, and reduce water and fertilizer consumption [27,28]. The previous protocols achieved the speed breeding of crops mainly through the regulation of the above-ground environment, such as the temperature and light, because these environmental factors are easier to control. The hydroponic cultivation of the PF system demonstrates that rice growth can be accelerated to achieve speed breeding by simultaneously regulating the above-ground environment and the underground rhizosphere environment. Hydroponics provides convenience for the precise control of the rhizosphere environment, including the temperature, DO, pH, and various nutritional elements such as nitrogen (N), phosphorus (P), and potassium (K) [12], compared with conventional pot cultivation. The suitable rhizosphere environment and adequate nutrient supply promote the speed-breeding protocol to achieve faster generation advancement [29]. Moreover, the multilayer PF system expands the utilization area through vertical cultivation, allowing more crops to be planted in order to reduce high operating costs and energy consumption per unit area in fully controlled facilities.

3.2. Differentiation of PF- and field-cultivated rice seeds via spectral analysis

The main components of rice seeds, such as moisture, starch, fat, protein, and various amino acids, have a large number of hydrogen-encompassing groups (X–H) with infrared absorption ability [30]. Recently, ATR-IR and its spectra were applied to identify rice seeds based on PCA, OPLS-DA, and other pattern-recognition methods [30]. Thus, to realize the high-precision identification of rice seeds, we collected the ATR-IR spectra at 400–4000 cm^{-1} and the HSI spectra at 400–1000 cm^{-1} of the rice seeds and further established PCA and OPLS-DA models to differentiate the PF- and field-cultivated rice seeds.

The results of the ATR-IR spectra indicated that the absorption spectra of the different rice seeds were similar, at around 400–4000 cm^{-1}, exhibiting five major bands at wavelengths of 1150–1220, 1410–1500, 1660–1800, 2860–2951, and 2975–3650 cm^{-1} (Figs. 3(a) and (b)). The 1150–1220 cm^{-1} band can be attributed to the C–H second overtone corresponding to aliphatic hydrocarbons, while the 1410–1500 cm^{-1} band can be attributed to the O–H functional group related to starch or the N–H first overtone related to protein [17]. For water, distinctively negative absorption bands at 1660–1800 and 2975–3650 cm^{-1} are associated with the O–H bending [31]. Aromatic compounds show absorption peaks at 1042 cm^{-1} due to the C–H bending vibrations in the aromatic surface of the benzene ring. For carboxylic acids, the most characteristic peak is located at 1085 cm^{-1} and is due to the C=O (carboxyl) stretch in –COOH. Absorption bands at the 2860–2951 cm^{-1} region can also be related to alkanes, alcohols, and fatty acids due to the C–H stretching in CH$_3$ and CH$_2$ groups. The data revealed that the absorption peaks of water, aromatic compounds, alkanes, alcohols, fatty acids, and carboxylic acids dominated the spectra, indicating that these may be the major compounds in the rice seeds. The characteristic bands observed at 965 and 1500 cm^{-1} can be attributed to sugars and organic acids and are due to CH–OH stretching. The distinctively negative absorption bands at 1410–1450 and 1510–1540 cm^{-1} can be attributed to N–H, C–H, and O–H stretching in proteins and amino acids [31]. To further understand the intrinsic variation in the two types of rice seeds, we performed a PCA on the ATR-IR spectra data at 400–4000 cm^{-1} (Fig. 3(c)), which showed a clear separation between the PF- and field-cultivated rice seeds. As shown in Fig. 3(d), the OPLS-DA model revealed a more pronounced distinc-

Fig. 3. Average ATR-IR and HSI of PF- and field-cultivated rice seeds. (a) Average ATR-IR at 400–2500 cm^{-1}; (b) average ATR-IR at 2500–4000 cm^{-1}; (c) PCA at 400–4000 cm^{-1}; (d) OPLS-DA at 400–4000 cm^{-1}; (e) average HSI at 400–750 cm^{-1}; (f) average HSI at 750–1000 cm^{-1}; (g) PCA of HSI at 400–1000 cm^{-1}; (h) OPLS-DA of HSI at 400–1000 cm^{-1}.

tion between the PF- and field-cultivated rice seed samples, with a cumulative contribution rate of 96% for principal component 1 (PC1) and principal component 2 (PC2). These results indicate the intrinsic variations between the two types of rice seeds.

The results of the HSI spectra revealed that the absorption spectra of the PF- and field-cultivated rice seeds were similar at around 400–750 cm^{-1} (Fig. 3(e)) but differed at around 750–1000 cm^{-1} (Fig. 3(f)). As shown in Fig. 3(g), the PCA of the HSI spectra at 400–1000 cm^{-1} showed a clear separation between the PF- and field-cultivated rice seeds, with PC1 and PC2 explaining 92% of the total variance. The OPLS-DA plot (Fig. 3(h)) showed a clearer separation between the PF- and field-cultivated rice seed samples, while the cumulative contribution rate of PC1 and PC2 was 64%.

In this way, the PF- and field-cultivated rice seeds were distinguishable according to their different spectral fingerprints, which were likely to be related to their chemical composition and abundance, in line with the results from previous studies [2,32]. Speed breeding techniques can influence the ATR-IR spectra of rice seeds, as detected by HSI and ATR-IR.

3.3. Influences of PF-based speed breeding on non-volatile metabolites of rice seeds

Speed breeding holds great significance for breaking through the bottleneck of traditional breeding and cultivation technology. However, its effects on the quality of the rice remain unclear. Therefore, we further investigated whether PF-based speed breeding could significantly influence the non-volatile metabolites in rice.

3.3.1. Analysis of the non-volatile metabolite profile

To explore the effects of speed breeding on the non-volatile metabolite profile of rice, a metabolomics analysis was performed based on UPLC-MS/MS (Fig. 4). A total of 1000 non-volatile differential metabolites were determined under both positive and negative ion modes, including 190 flavonoids, 171 lipids, 147 phenolic acids, 102 amino acids and derivatives, 97 alkaloids, 89 organic acids, 65 nucleotides and derivatives, 33 lignans and coumarins, ten terpenoids, two quinones, one tannin, and 93 other metabolites (Fig. S1(a) in Appendix A). All groups of metabolites were detected in both the PF- and field-cultivated rice seeds, but the proportion of metabolites in the PF-cultivated rice seeds differed from that in the field-cultivated rice seeds (Fig. 4(a)). In the field-cultivated rice seeds, amino acids and derivatives (28.20%), lipids (22.40%), and alkaloids (19.14%) were among the highest proportion of non-volatile metabolites, while lipids (22.84%), organic acids (20.97%), amino acids and derivatives (12.37%), and alkaloids (10.73%) were the main non-volatile metabolites in the PF-cultivated rice seeds.

As shown in Fig. 4(b), the total amounts of non-volatile metabolites in the PF-cultivated rice seeds were higher than those in the field-cultivated rice seeds. It has been reported that lipids play an important role in the firmness of cooked rice [33]. Compared with field-cultivated rice seeds, no significant difference in lipid levels was found between the PF- and field-cultivated rice seeds. Interestingly, we found that the relative abundances of phenolic acids and organic acids were significantly increased in the PF-cultivated rice seeds. Phenolic acids and organic acids are the intermediate metabolites of several amino acids for energy production and can improve the flavor, nutritional value, and storage time of food [34,35]. Since many organic acids and phenolic acids exhibit antioxidant activity [36,37], cultivation in a PF environment may enhance the antioxidant composition of rice, making it more nutritious. However, the relative abundances of amino acids in the PF-cultivated rice seeds were lower than those in the field-cultivated rice seeds, which may be associated with the biotransformation of amino acids into organic acids and phenolic acids during rice growth.

To further evaluate the overall metabolic diversity of the PF- and field-cultivated rice, the metabolomics data was analyzed through a PCA score plot, and it was found that the PC1 and PC2 respectively explained 63% and 10% of the total variance (Fig. 4(c)). A heatmap derived from the HCA analysis displayed the dynamic changes in the rice seeds during breeding (Fig. S1(b) in Appendix A). Based on the data, the samples were divided into two groups, consistent with the PCA and OPLS-DA results.
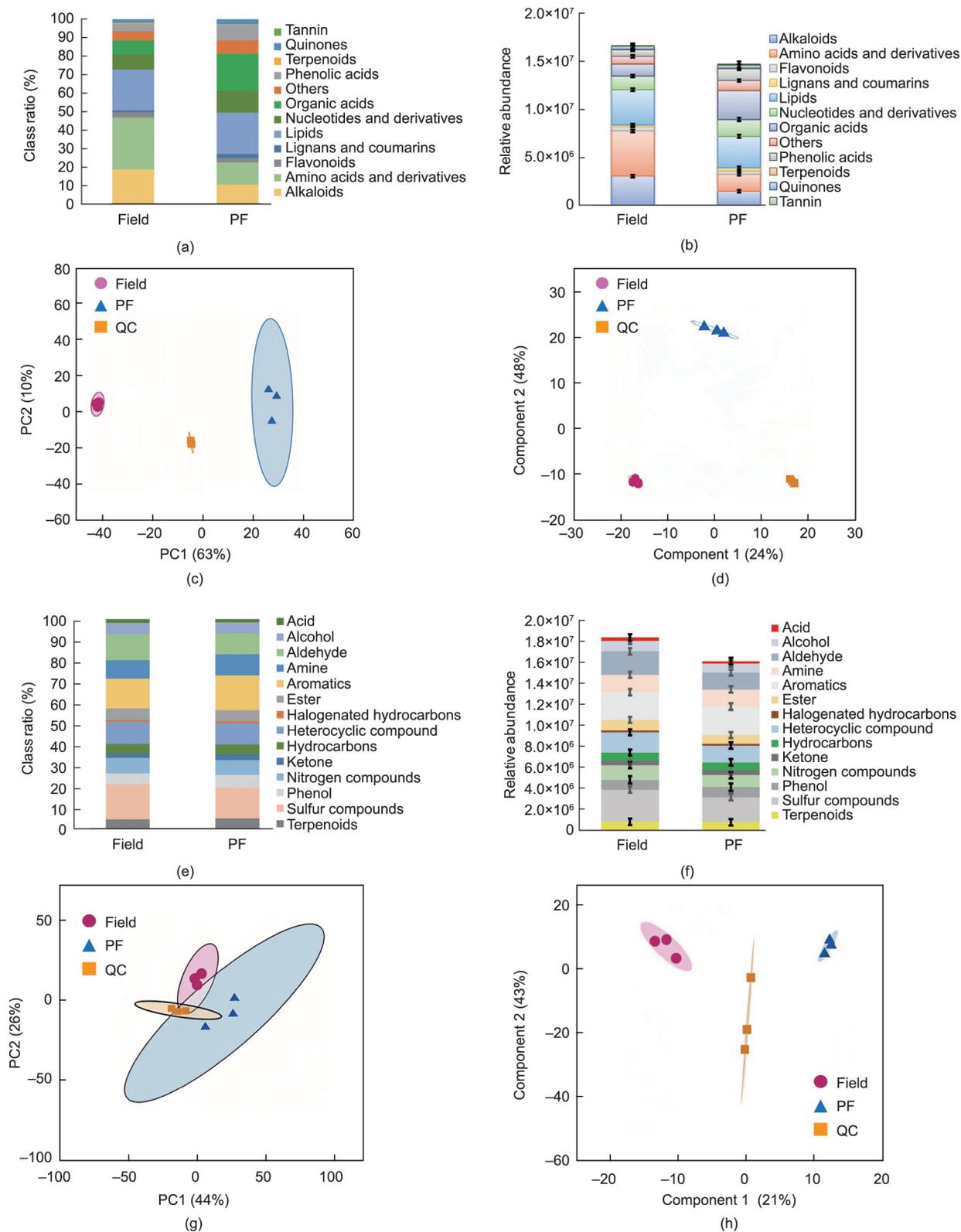
Overall, these results indicated that the PF environment influenced the non-volatile metabolic profiles of the rice seeds. It is worth noting that speed breeding could improve the nutritional value of indica rice in terms of increasing its organic acids and phenolic acids, probably from the biotransformation of amino acids.

3.3.2. Discovery of non-volatile differential metabolites

In the OPLS-DA evaluation model, the prediction parameters include R^2X, R^2Y, and Q^2. Specifically, R^2X and R^2Y respectively signify the explanatory power of the constructed model for the X and Y matrices, while Q^2 represents the predictive capability of the model. A higher proximity to 1 in these three indicators indicates greater stability and reliability in the model. An effective model can be considered when $Q^2 > 0.5$, whereas an excellent model is defined by $Q^2 > 0.9$. A predictable and non-overfitting OPLS-DA model ($R^2Y = 1$, $Q^2 = 0.992$) was verified and performed for screening differentially expressed compounds in the rice seeds. Based on the OPLS-DA plot (Fig. 4(d)) and the VIP values, a total of 426 differential metabolites ($p < 0.05$, VIP ≥ 1, FC ≥ 2, and FC ≤ 0.5) were identified as biomarkers responsible for the differentiation of PF- and field-cultivated rice seeds (Table S3 in Appendix A), including 68 flavonoids, 60 amino acids and their derivatives, 56 alkaloids, 48 phenolic acids, 34 nucleotides and their derivatives, 13 lignans and coumarins, 22 lipids, 23 organic acids, four triterpenes, and 29 others. Among them, 257 differential metabolites were up-regulated, while 169 differential metabolites were down-regulated. The first 20 metabolites with the top VIP values in the OPLS-DA model are shown in Fig. 5(a).

Compared with those in the field-cultivated rice seeds, 157 differential metabolites were discovered in the PF-cultivated rice seeds (VIP ≥ 1.00 and $p < 0.05$) (Table S4 in Appendix A), including 68 up-regulated metabolites (13 phenolic acids, ten lipids, eight organic acids, seven nucleotides and their derivatives, seven flavonoids, five alkaloids, five lignans and coumarins, one terpenoid, and 12 others) (Fig. 5(b)). Among the 68 significantly up-regulated non-volatile metabolites, eight non-volatiles were only detected in the PF-cultivated rice seeds, including pinoresinol-4-*O*-glucoside, 2-α-linolenoyl-glycerol-1-*O*-glucoside, 3′-deoxyadenosine, 6-*O*-caffeoyl-*D*-glucose, 1-*O*-caffeoyl-*β*-*D*-glucose, 3-indolepropionic acid (3-IPA), kaempferol-4′-*O*-glucoside, and isolariciresinol 9′-*O*-glucoside. Notably, pinoresinol-4-*O*-glucoside, a lignan compound, is also found in the flower of *S. japonicas* [38] and *Forsythiae Fructus* [39], and has possible analgesic effects. 3′-Deoxyadenosine is a nucleoside analogue with anticancer properties against several types of cancer [40], while 1-*O*-caffeoyl-*β*-*D*-glucose is a hydrophilic antioxidant separated from the fruits of the vegetable *Luffa cylindrica* (L.) Roem (i.e., sponge gourd) [41]. 3-IPA, a tryptophan-derived metabolite, has multiple beneficial functions, such as immune regulation and anti-inflammatory and antioxidant activities [42,43]. Interestingly, isololiolide was the only up-regulated terpenoid found among them; it is also found in *Portulaca oleracea* L. and has plausible medical applications against certain neurodegenerative disorders [44,45]. On the other hand, all 20 amino acids and derivatives were significantly down-regulated (Fig. 5(c)).
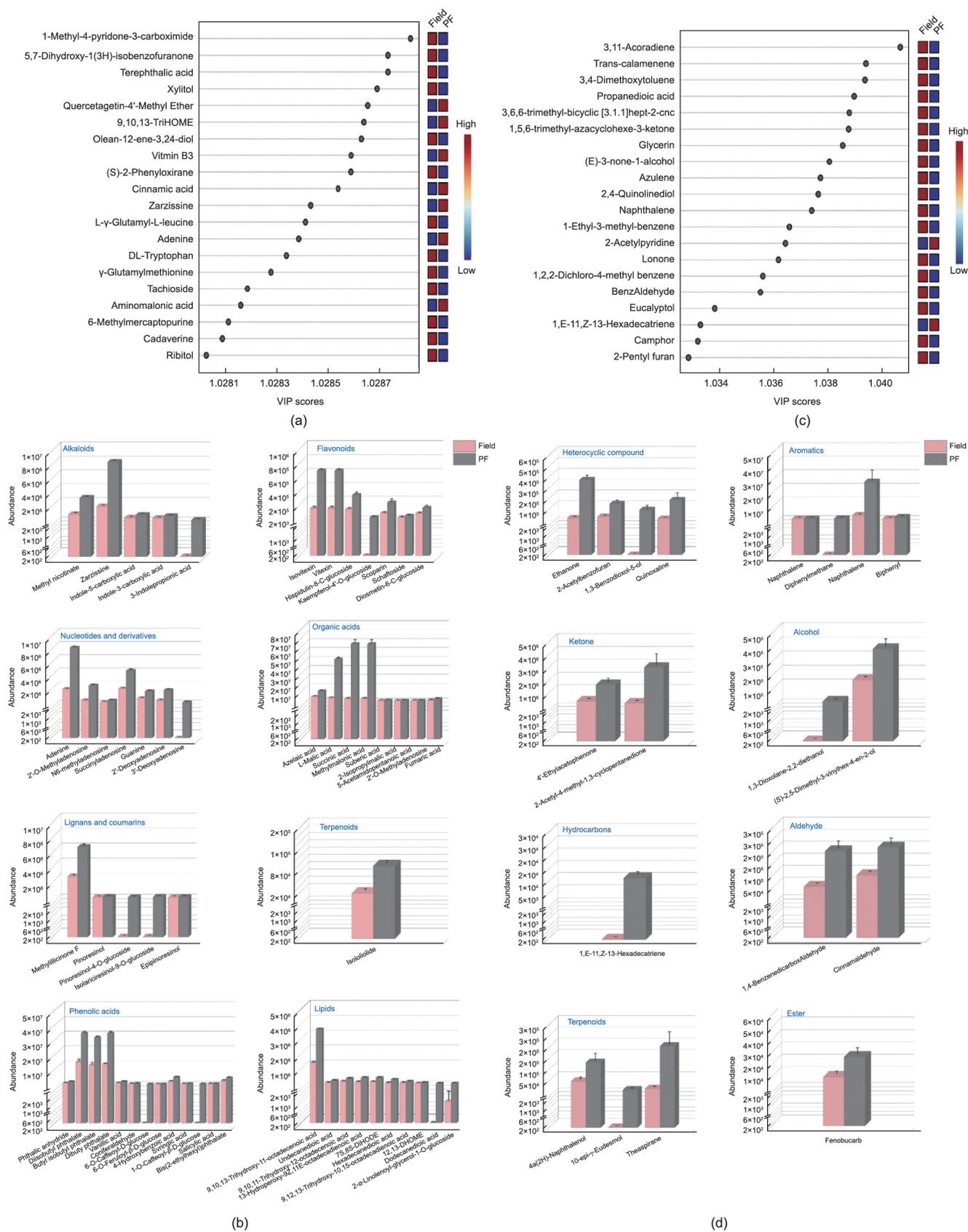
To elucidate the dominant metabolic pathways for the non-volatile metabolites, we annotated and enriched the 426 differential non-volatile metabolites and divided them into different KEGG pathways. The differential metabolites were involved in 89 pathways; the top 20 pathways ($p < 0.05$) were illustrated in bubble plots (Fig. S2(a) in Appendix A), including the pathways of aminoacyl-transfer RNA (tRNA) biosynthesis; glutathione metabolism; biosynthesis of amino acids; glycine, serine, and threonine

Fig. 4. Comparison of the non-volatile and volatile differential metabolite profiles of the PF- versus field-cultivated rice seeds. (a) Class ratio of 1000 non-volatile metabolites; (b) relative abundance of different types of the 1000 non-volatile metabolites; (c) PCA of 1000 non-volatile metabolites; (d) OPLS-DA of 1000 non-volatile metabolites; (e) class ratio of 530 volatile metabolites; (f) relative abundance of different types of the 530 volatile metabolites; (g) PCA of 530 volatile metabolites; (h) OPLS-DA of 530 volatile metabolites.

metabolism; and arginine and proline metabolism. These pathways are mainly associated with the metabolism of alkaloids, flavonoids, lignans and coumarins, lipids, nucleotides, organic acids, phenolic acids, terpenoids, and amino acids.

The main metabolic pathways of the 68 significantly up-regulated differential metabolites and 20 significantly down-regulated amino acids and derivatives are integrated in Fig. S3 in Appendix A. Ultimately, 34 compounds (11 amino acids and derivatives, five organic

Fig. 5. Comparison of key differential non-volatile and volatile metabolites in PF- and field-cultivated rice seeds. (a) 20 non-volatile differential metabolites with the top VIP value in the OPLS-DA model; (b) 68 up-regulated non-volatile metabolites and 20 down-regulated amino acids and derivatives (VIP ≥ 1.00, $p < 0.05$, and level = 1); (c) 20 volatile differential volatiles with the top VIP values in the OPLS-DA model; (d) 19 up-regulated differential volatiles (VIP ≥ 1.00, $p < 0.05$, and level = 1). DiHODE: 8S-dihydroxy-9Z,12Z-octadecadienoic acid; DHOME: dihydroxyoctadec-9-enoic acid.

acids, three lipids, three nucleotides and their derivatives, three phenolic acids, two flavonoids, one lignan, and six others) were annotated in 52 related KEGG pathways (Table S5 in Appendix A). It was found that the organic acids and phenolic acids were closely related to the pathways of pyrimidine metabolism; pyruvate metabolism; alanine, aspartate, and glutamate metabolism; and phenylpropanoid biosynthesis. On the other hand, 11 amino acids and derivatives were closely associated with the amino acid biosynthesis, aminoacyl-tRNA biosynthesis, and glyoxylate dicarboxylate metabolism pathways. The remaining 45 up-regulated differential metabolites and nine down-regulated amino acids and derivatives were not annotated in any pathways due to a lack of available information about their functions.

Taken together, these data suggest that PF cultivation can induce rice to accumulate more organic acids and phenolic acids than field cultivation, which might be related to promotion of the pyrimidine metabolism, pyruvate metabolism, alanine, aspartate and glutamate metabolism, and phenylpropanoid biosynthesis under PF conditions. The 68 significantly up-regulated differential metabolites and 20 significantly down-regulated amino acids and derivatives can be used as non-volatile biomarkers to differentiate PF-cultivated rice seeds from field-cultivated rice seeds.

3.4. Influences of PF-based speed breeding on volatile metabolites of rice seeds

Volatile metabolites are the main chemical compounds that determine the characteristic aroma and flavor of foods, making them another important indicator of rice quality [46,47]. Therefore, we also investigated whether PF-based speed breeding could significantly influence the volatile metabolites of rice.

3.4.1. The difference in composition of volatile compounds

A total of 530 volatile metabolites were determined based on the GC-MS system under both positive and negative ion modes. All these volatile compounds could be classified into 15 classes (Fig. S1(c) in Appendix A): 93 heterocyclic compounds (17.58%), 91 esters (17.2%), 77 terpenoids (14.56%), 58 hydrocarbons (10.96%), 49 aldehydes (9.07%), 46 alcohols (8.70%), 38 ketones (7.18%), 35 aromatics (6.62%), 13 acids (2.46%), nine phenols (1.70%), seven amines (1.32%), six nitrogen compounds (1.13%), four halogenated hydrocarbons (0.76%), two sulfur compounds (0.38%), and two other compounds (0.38%). As shown in Fig. 4(e), the class ratio of volatile compounds was similar in the two groups of PF- and field-cultivated rice seeds. In the PF-cultivated rice seeds, the most abundant volatile metabolites included aromatics (16.66%), sulfur compounds (14.85%), heterocyclic compounds (10.08%), and amines (10.11%). In contrast, the most abundant volatile metabolites in the field-cultivated rice seeds were sulfur compounds (16.70%), aromatics (14.29%), aldehydes (12.42%), and heterocyclic compounds (10.52%). As shown in Fig. 4(f), the total amount of volatiles in the PF-cultivated rice seeds was lower than that in the field-cultivated rice seeds, while there was a significant increase in the accumulation of phenols, ketones, aromatics, and amines in the PF-cultivated rice seeds—probably associated with the special breeding conditions in the PF. We then conducted a PCA analysis. In the PCA score plot, PC1 and PC2 explained 44% and 26% of the total variance, respectively (Fig. 4(g)). Moreover, two main clusters were obtained based on the HCA map of the 530 volatile metabolites (Fig. S1(d) in Appendix A). Taken together, these results reveal the composition and distribution of the volatile metabolites in the rice seeds, as well as highlight the differences between PF-cultivated rice and field-cultivated rice. This insight provides important information for the further study of rice quality characteristics and cultivation conditions.

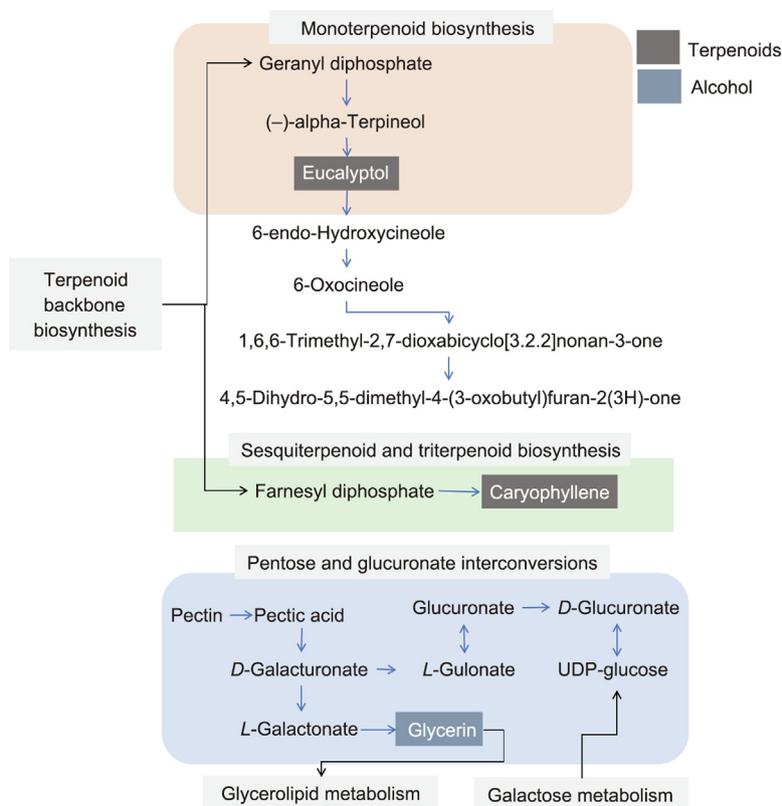#### 3.4.2. The contribution of volatile compounds to flavor profiles

An OPLS-DA model (R^2Y = 0.995, Q^2 = 0.910) was performed and verified for screening the differential volatile compounds in the rice seeds. Based on the OPLS-DA plot (Fig. 4(h)) and the VIP values, a total of 74 metabolites ($p < 0.05$, VIP $\geq$ 1, FC $\geq$ 2, and FC $\leq$ 0.5) were identified as biomarkers responsible for the differentiation of the PF- and field-cultivated rice seeds. A total of 74 top differential metabolites (19 terpenoids, 13 heterocyclic compounds, ten aromatics, eight ketones, seven esters, seven aldehydes, seven alcohols, one acid, one hydrocarbon, and one nitrogen compound) were discovered, with 28 metabolites being up-regulated and 46 metabolites down-regulated. The first 20 differential metabolites with top VIP values in the OPLS-DA model are shown in Fig. 5(c).

Furthermore, compared with the field-cultivated rice seeds, 65 top differential metabolites were discovered in the PF-cultivated rice seeds (VIP $\geq$ 1.00, $p < 0.05$, and level = 1) (Table S6 in Appendix A), including 17 terpenoids, ten heterocyclic compounds, nine aromatics, seven ketones, five esters, seven aldehydes, seven alcohols, one acid, one hydrocarbon, and one nitrogen compound. Among the 65 metabolites, 19 significantly up-regulated volatile metabolites were identified in both the PF- and FT-cultivated rice seeds, including four heterocyclic compounds, four aromatics, three terpenoids, two ketones, two alcohols, two aldehydes, one hydrocarbon, and one ester (Fig. 5(d)). Notably, five volatiles (1,3-benzodioxol-5-ol, diphenylmethane, 1,E-11,Z-13-hexadecatriene, 1,3-dioxolane-2,2-diethanol, and 10-epi-γ-eudesmol) were only detected in the PF-cultivated rice seeds. 1,3-benzodioxol-5-ol—also known as sesamol—is a powerful functional food ingredient with multiple beneficial functions, including cardioprotection [48], anti-neuroinflammation [49], and anti-asthma activity [50].
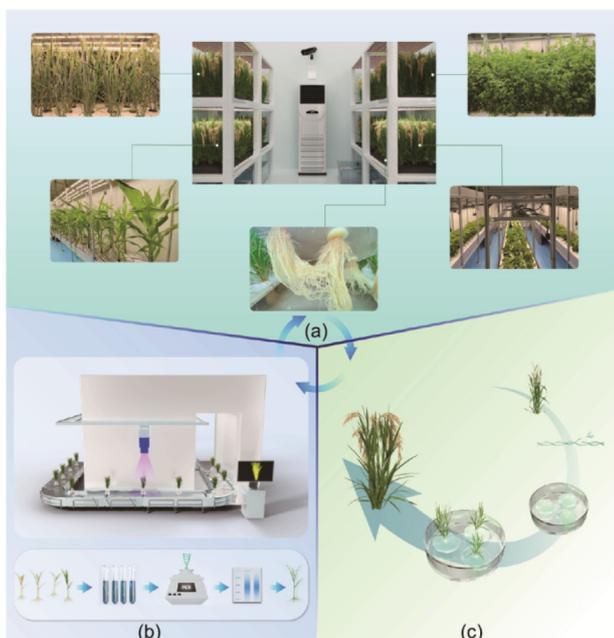
The 74 differential metabolites were then subjected to KEGG analysis, and ten pathways were identified, including pathways related to monoterpenoid, secondary metabolites, and sesquiterpenoid and triterpenoid biosynthesis, which are illustrated in Fig. S2(b) in Appendix A. Among the 19 up-regulated metabolites, seven compounds (e.g., two terpenoids and one alcohol) were annotated in the related KEGG pathways (Fig. 6), while the remaining 58 compounds were not annotated due to limited information about their functions (Table S7 in Appendix A).

4. Conclusions and future directions

With the continuous growth of the world's population, increasing the rate of crop genetic improvement presents a great challenge. We have established a vertical multilayer cultivation system with hydroponics in a PF to achieve the speed breeding of rice, shortening the growth period of its field cultivation almost by half, which should result in an annual yield of 5–6 generations of rice. The PF system realizes the integrated regulation of the above-ground growing environment and the underground rhizosphere environment, making it possible to achieve faster generation advancement for crops. In addition, multilayer cultivation provides greater space utilization and energy efficiency per unit area than single-layer cultivation and can thus effectively address the issue of the cost of the high consumption of energy (e.g., electricity), thereby promoting the economic sustainability of speed breeding in PFs. As a flexible speed-breeding platform, the PF system can be used for the speed breeding of not only rice but also crops such as wheat, soybean, corn, and alfalfa, allowing rapid generation advancement. Furthermore, the PF system can be combined with modern breeding technologies such as high-throughput crop phenotype (HCP), molecular marker-assisted selection (MAS), and clustered regularly interspaced short palindromic repeats(CRISPR)-associated protein 9 (Cas9) gene editing to construct a new fast and precise breeding system, by which

Fig. 6. The metabolic relationships among 19 up-regulated volatile compounds. Overall, these results indicate that PF cultivation has significant impacts on the volatiles in rice seeds, and the application of PF breeding can enhance the flavor qualities of indica rice by increasing its levels of certain phenols, ketones, aromatics, and amines. UDP-glucose: urine diphosphate glucose.

Fig. 7. An innovative breeding strategy integrating the PF system with modern breeding technologies. (a) The PF speed-breeding platform; (b) a precise selection platform with MAS and HCP; (c) molecular design breeding of crops. PCR: polymerase chain reaction.

the whole breeding process can be rapidly completed locally, compared with shuttle breeding (Fig. 7).

It was found that lipids, organic acids, amino acids, and alkaloids were the top four classes of metabolites in the PF-cultivated rice seeds. More phenolic acids and organic acids—but less amino

acids and derivatives—were accumulated in PF-cultivated rice seeds in comparison with the field-cultivated seeds. In addition, more volatiles—including phenols, ketones, aromatics, and amines—were generated in the PF-cultivated rice seeds. Compared with the field-cultivated rice seeds, eight non-volatiles and five volatiles were only detected in the PF-cultivated rice seeds, making these compounds potential biomarkers for characterizing the rice-breeding progress in a PF. Overall, this study underscores the potential of PF systems to not only improve rice-breeding efficiency but also enhance the nutritional quality of rice. By leveraging innovative technologies and cultivation methods, such as PF systems, we can address the challenges posed by population growth and climate change to ensure food production in the future.

CRediT authorship contribution statement

Yi Liu: Writing – original draft, Software, Methodology, Formal analysis, Data curation. **Zong-Geng Li:** Writing – review & editing,

Resources, Methodology. **Hao Cheng:** Software, Methodology. **Xiao Yang:** Validation, Software. **Ming-Yue Li:** Methodology, Data curation. **Hong-Yan Liu:** Writing – review & editing, Supervision, Conceptualization. **Ren-You Gan:** Writing – review & editing, Visualization, Supervision, Resources. **Qi-Chang Yang:** Funding acquisition.

Declaration of competing interest

The authors declare that they have no known competing financial interests or personal relationships that could have appeared to influence the work reported in this paper.

Appendix A. Supplementary data

Supplementary data to this article can be found online at https://doi.org/10.1016/j.eng.2024.09.019.

References

[1] Bandumula N. Rice production in Asia: key to global food security. Proc Natl Acad Sci, India, Sect B Biol Sci 2018;88(4):1323–8.
[2] Song EH, Jeong J, Park CY, Kim HY, Kim EH, Bang E, et al. Metabotyping of rice (*Oryza sativa* L.) for understanding its intrinsic physiology and potential eating quality. Food Res Int 2018;111:20–30.
[3] Zhang L, Cui D, Ma X, Han B, Han L. Comparative analysis of rice reveals insights into the mechanism of colored rice via widely targeted metabolomics. Food Chem 2023;399:133926.
[4] Jin R, Zhang C, Jia L, Tang Q, Gao L, Zhao G, et al. Identification of rice seed varieties based on near-infrared hyperspectral imaging technology combined with deep learning. ACS Omega 2022;7(6):4735–49.
[5] Kim DS, Kim QW, Kim H, Kim HJ. Changes in the chemical, physical, and sensory properties of rice according to its germination rate. Food Chem 2022;388:133060.
[6] Hickey LT, Hafeez AN, Robinson H, Jackson SA, Leal-Bertioli SCM, Tester M, et al. Breeding crops to feed 10 billion. Nat Biotechnol 2019;37(7):744–54.
[7] Voss-Fels KP, Stahl A, Hickey LT. Q&A: modern crop breeding for future food security. BMC Biol 2019;17:18.
[8] Zhang L, Yang X, Li T, Gan R, Wang Z, Peng J, et al. Plant factory technology lights up urban horticulture in the post-coronavirus world. Hortic Res 2022;9:uhac018.
[9] De La Fuente GN, Frei UK, Lübberstedt T. Accelerating plant breeding. Trends Plant Sci 2013;18(12):667–72.
[10] Ghosh S, Watson A, Gonzalez-Navarro OE, Ramirez-Gonzalez RH, Yanes L, Mendoza-Suárez M, et al. Speed breeding in growth chambers and glasshouses for crop breeding and model plant research. Nat Protoc 2018;13(12):2944–63.
[11] Nagatoshi Y, Fujita Y. Accelerating soybean breeding in a CO$_2$-supplemented growth chamber. Plant Cell Physiol 2019;60(1):77–84.
[12] Zhang L, Huang L, Li T, Wang T, Yang X, Yang Q. The skyscraper crop factory: a potential crop-production system to meet rising urban food demand. Engineering 2023;31:70–5.
[13] Thongtip A, Mosaleeyanon K, Korinsak S, Toojinda T, Darwell CT, Chutimanukul P, et al. Promotion of seed germination and early plant growth by KNO$_3$ and light spectra in *Ocimum tenuiflorum* using a plant factory. Sci Rep 2022;12(1):6995.
[14] Watson A, Ghosh S, Williams MJ, Cuddy WS, Simmonds J, Rey MD, et al. Speed breeding is a powerful tool to accelerate crop research and breeding. Nat Plants 2018;4(1):23–9.
[15] Jähne F, Hahn V, Würschum T, Leiser WL. Speed breeding short-day crops by LED-controlled light schemes. Theor Appl Genet 2020;133(8):2335–42.
[16] Kabade PG, Dixit S, Singh UM, Alam S, Bhosale S, Kumar S, et al. SpeedFlower: a comprehensive speed breeding protocol for *indica* and *japonica* rice. Plant Biotechnol J 2024;22(5):1051–66.
[17] John R, Bhardwaj R, Jeyaseelan C, Bollinedi H, Singh N, Harish GD, et al. Germplasm variability-assisted near infrared reflectance spectroscopy chemometrics to develop multi-trait robust prediction models in rice. Front Nutr 2022;9:946255.
[18] Song T, Das D, Zhu F, Chen X, Chen M, Yang F, et al. Effect of alternate wetting and drying irrigation on the nutritional qualities of milled rice. Front Plant Sci 2021;12:721160.
[19] Wang C, Feng Y, Zhang S, Fu T, Sheng Y, Zhang Y, et al. Effects of storage on brown rice (*Oryza sativa* L.) metabolites, analyzed using gas chromatography and mass spectrometry. Food Sci Nutr 2020;8(6):2882–94.
[20] Guo L, Yu Y, Yu H, Tang Y, Li J, Du Y, et al. Rapid quantitative analysis of adulterated rice with partial least squares regression using hyperspectral imaging system. J Sci Food Agric 2019;99(12):5558–64.
[21] Liu W, Zeng S, Wu G, Li H, Chen F. Rice seed purity identification technology using hyperspectral image with lasso logistic regression model. Sensors 2021;21(13):4384.
[22] Liu Y, Liu HY, Xia Y, Guo H, He XQ, Li H, et al. Screening and process optimization of ultrasound-assisted extraction of main antioxidants from sweet tea (*Lithocarpus litseifolius* [Hance] Chun). Food Biosci 2021;43:101277.
[23] Zeng T, Fang B, Huang F, Dai L, Tang Z, Tian J, et al. Mass spectrometry-based metabolomics investigation on two different indica rice grains (*Oryza sativa* L.) under cadmium stress. Food Chem 2021;343:128472.
[24] Alahmad S, Dinglasan E, Leung KM, Riaz A, Derbal N, Voss-Fels KP, et al. Speed breeding for multiple quantitative traits in durum wheat. Plant Methods 2018;14:36.
[25] Chiurugwi T, Kemp S, Powell W, Hickey LT. Speed breeding orphan crops. Theor Appl Genet 2019;132(3):607–16.
[26] Cazzola F, Bermejo CJ, Gatti I, Cointry E. Speed breeding in pulses: an opportunity to improve the efficiency of breeding programs. Crop Pasture Sci 2021;72(3):165–72.
[27] Van Delden SH, SharathKumar M, Butturini M, Graamans LJA, Heuvelink E, Kacira M, et al. Current status and future challenges in implementing and upscaling vertical farming systems. Nat Food 2021;2(12):944–56.
[28] Ahn TI, Park JE, Jung JH, Kim SM, Yoo G, Kim HS, et al. Nutrient dosing framework for an emission-free urban hydroponic production. Front Plant Sci 2021;12:768717.
[29] Zhang S, Zhang Y, Li K, Yan M, Zhang J, Yu M, et al. Nitrogen mediates flowering time and nitrogen use efficiency via floral regulators in rice. Curr Biol 2021;31(4):671–683.e5.
[30] Chen J, Li M, Pan T, Pang L, Yao L, Zhang J. Rapid and non-destructive analysis for the identification of multi-grain rice seeds with near-infrared spectroscopy. Spectrochim Acta A Mol Biomol Spectrosc 2019;219:179–85.
[31] Wu Z, Xu E, Long J, Pan X, Xu X, Jin Z, et al. Comparison between ATR-IR, Raman, concatenated ATR-IR and Raman spectroscopy for the determination of total antioxidant capacity and total phenolic content of Chinese rice wine. Food Chem 2016;194:671–9.
[32] Li F, Liu Y, Zhang X, Liu L, Yan Y, Ji X, et al. Transcriptome and metabolome analyses reveals the pathway and metabolites of grain quality under *phytochrome B* in rice (*Oryza sativa* L.). Rice 2022;15(1):52.
[33] Concepcion J, Calingacion M, Garson MJ, Fitzgerald MA. Lipidomics reveals associations between rice quality traits. Metabolomics 2020;16(5):54.
[34] Ramsay J, Morton J, Norris M, Kanungo S. Organic acid disorders. Ann Transl Med 2018;6(24):472.
[35] Shi Y, Pu D, Zhou X, Zhang Y. Recent progress in the study of taste characteristics and the nutrition and health properties of organic acids in foods. Foods 2022;11(21):3408.
[36] Zhang B, Xia T, Duan W, Zhang Z, Li Y, Fang B, et al. Effects of organic acids, amino acids and phenolic compounds on antioxidant characteristic of Zhenjiang aromatic vinegar. Molecules 2019;24(20):3799.
[37] Tyagi A, Lim MJ, Kim NH, Barathikannan K, Vijayalakshmi S, Elahi F, et al. Quantification of amino acids, phenolic compounds profiling from nine rice varieties and their antioxidant potential. Antioxidants 2022;11(5):839.
[38] He L, Zhou Y, Wan G, Wang W, Zhang N, Yao L. Antinociceptive effects of flower extracts and the active fraction from *Styrax japonicus*. J Ethnopharmacol 2022;284:114779.
[39] Zhang F, Li Z, Li C, Li M, Yao Z, Yao X, et al. Characterization of lignans in *Forsythiae* Fructus and their metabolites in rats by ultra-performance liquid chromatography coupled time-of-flight mass spectrometry. J Pharm Pharmacol 2020;72(12):1879–92.
[40] Lee S, Alaali L, Kwon HJ, Rigi M, Eberhart CG. Cordycepin (3′-deoxyadenosine) suppresses heat shock protein 90 function and targets tumor growth in an adenosine deaminase-dependent manner. Cancers 2022;14(13):3122.
[41] Du Q, Xu Y, Li L, Zhao Y, Jerz G, Winterhalter P. Antioxidant constituents in the fruits of *Luffa cylindrica* (L.) Roem. J Agric Food Chem 2006;54(12):4186–90.
[42] Owumi SE, Najophe ES, Otunla MT. 3-Indolepropionic acid prevented chlorpyrifos-induced hepatorenal toxicities in rats by improving anti-inflammatory, antioxidant, and pro-apoptotic responses and abating DNA damage. Environ Sci Pollut Res Int 2022;29(49):74377–93.
[43] Guijas C, Horton LE, Hoang L, Domingo-Almenara X, Billings EM, Ware BC, et al. Microbial metabolite 3-indolepropionic acid mediates immunosuppression. Metabolites 2022;12(7):645.
[44] Baruah V, Paul R, Gogoi D, Mazumder N, Chakraborty S, Das A, et al. Integrated computational approach toward discovery of multi-targeted natural products from Thumbai (*Leucas aspera*) for attuning NKT cells. J Biomol Struct Dyn 2020;40(7):2893–907.
[45] Xu W, Wang J, Ju B, Lan X, Ying X, Stien D. Seven compounds from *Portulaca oleracea* L. and their anticholinesterase activities. Nat Prod Res 2022;36(10):2547–53.
[46] Lee J, Kim DW, Jang GJ, Song S, Park KJ, Lim JH, et al. Effects of different storage conditions on the metabolite and microbial profiles of white rice (*Oryza sativa* L.). Food Sci Biotechnol 2019;28(3):623–31.
[47] Mihaylova D, Popova A, Vrancheva R, Dincheva I. HS-SPME-GC–MS volatile profile characterization of peach (*Prunus persica* L. Batsch) varieties grown in the eastern Balkan peninsula. Plants 2022;11(2):166.
[48] Jayaraj P, Narasimhulu CA, Rajagopalan S, Parthasarathy S, Desikan R. Sesamol: a powerful functional food ingredient from sesame oil for cardioprotection. Food Funct 2020;11(2):1198–210.
[49] Feng X, Chen X, Zaeem M, Zhang W, Song L, Chen L, et al. Sesamol attenuates neuroinflammation by regulating the AMPK/SIRT1/NF-κB signaling pathway after spinal cord injury in mice. Oxid Med Cell Longev 2022;2022:8010670.
[50] Liou C, Chen YL, Yu MC, Yeh KW, Shen SC, Huang WC. Sesamol alleviates airway hyperresponsiveness and oxidative stress in asthmatic mice. Antioxidants 2020;9(4):295.